Supporting Information

Glutathione from recovered glucose as ingredient in antioxidant nanocapsules for triggered flavor delivery

Claudia Tallian[†], Vanessa Rumpler[†], Lukas Skopek[‡], Hannes Russmayer[§], Matthias G. Steiger[‡,§], Robert Vielnascher[†,‡], Simone Weinberger[‡], Alessandro Pellis[$], Sara Vecchiato[‡],and Georg M. Guebitz[†,‡]*

[†]University of Natural Resources and Life Sciences, Vienna (BOKU), Institute for Environmental Biotechnology, Department for Agrobiotechnology (IFA-Tulln), Konrad-Lorenz-Strasse 20, 3430 Tulln an der Donau, Austria.

[‡]Austrian Centre of Industrial Biotechnology, Division Enzymes & Polymers, Konrad-Lorenz-Strasse 20, 3430 Tulln an der Donau, Austria.

[§]University of Natural Resources and Life Sciences, Department of Biotechnology, Muthgasse 18, 1190 Vienna, Austria.

[$]University of York, Department of Chemistry, Green Chemistry Centre of Excellence, Heslington, York, Y010 5DD, United Kingdom

[*] Corresponding Author: sara.vecchiato@acib.at

Number of pages in the supporting information: 10

Number of figures in the supporting information: 6

Number of tables in the supporting information: 7

Table S1. Composition of WMVIII medium

Substance	Amount/Volume per 1 L
Glucose monohydrate	22 g
$NH_4H_2PO_4$	0.25 g
NH_4Cl	2.8 g
$MgCl_2 \cdot 6H_2O$	0.25 g
$CaCl_2 \cdot 2H_2O$	0.1 g
KH_2PO_4	2.0 g
$MgSO_4 \cdot 7H_2O$	0.55 g
Myo-Inositol	0.075 g
Sodium glutamate monohydrate	10 g
Trace salt solution*	4 mL
Vitamin solution**	4 mL

* Trace salts stock solution contained per 50 mL: 21.88 mg $ZnSO_4 \cdot 7H_2O$, 6.25 mg $Fe_2SO_4 \cdot 7H_2O$, 1.25 mg $CuSO_4 \cdot 5H_2O$, 1.25 mg $MnCl_2 \cdot 4H_2O$, 1.25 mg $Na_2MoO_4 \cdot 2H_2O$, 146.1 mg EDTA

**Vitamin solution contained per 50 mL: 125 mg nicotinic acid, 312.5 mg pyridoxal hydrochloride, 125 mg thiamine hydrochloride, 31.25 mg biotin, 625 mg calcium pantothenate

Table S2. HPLC gradient for determination of L-glutathione incorporation, where A is 20 mM NFPA and 0.6% TFA, B is 20 mM NFPA and 0.8% TFA and C is ACN.

Time [min]	A [%]	B [%]	C [%]
0	0	100	0
10	0	85	15
11.5	83.6	0	16.4
20	74	0	26
30	50	0	50
40	50	0	50
45	0	0	100
50	0	0	100
51	100	0	0

Table S3. HPLC gradient for the determination of RK, where A is ultrapure water, B is methanol and C is 10% formic acid in ultrapure water.

Time [min]	A [%]	B [%]	C [%]
0	85	5	10
1	80	10	10
8	40	50	10
10	0	100	0

Table S4. Independent factors of the 2^3 full factorial design (DoE 1) and the corresponding experimental averaged results for zeta potential (ZP) in mV and hydrodynamic radius (Radius) in nm, whereby 3 factors were defined: protein addition (qualitative; PRO), concentration of glutathione (quantitative, 1 to 10 $mg*mL^{-1}$; GLU) and the number of purification steps (quantitative, 1 to 10; PUR). Values in blot were excluded from the model analysis as outliers.

		Factors			Responses	
Exp No	**Run Order**	**PRO**	**GLU**	**PUR**	**ZP**	**Radius**
1	3	Yes	1	1	-13.02	476.104
2	2	No	1	1	-14.64	419.197
3	8	Yes	10	1	-12.49	578.045
4	4	No	10	1	-13.51	494.444
5	9	Yes	1	10	-13.78	425.593
6	6	No	1	10	-12.47	664.014
7	7	Yes	10	10	-13.16	353.877
8	1	No	10	10	-11.08	558.215
9	11	Yes	5.5	5	-13.37	513.014
10	10	Yes	5.5	5	-13.1	535.647
11	5	Yes	5.5	5	-13.29	**594.788**

Table S5. Independent factors of the central composite face-centered design (CCF; DoE 2) and the corresponding experimental averaged results for zeta potential (ZP) in mV and hydrodynamic radius (Radius) in nm, whereby 2 factors were defined: concentration of glutathione (quantitative, 1 to 10 mg*mL^{-1}; GLU) and the number of purification steps (quantitative, 1 to 5; PUR). Values in blot were excluded from the model analysis as outliers.

		Factors		Responses	
Exp No	**Run Order**	**GLU**	**PUR**	**ZP**	**Radius**
1	7	1	1	-12.68	282.311
2	5	10	1	-11.87	405.927
3	6	1	5	-12.71	314.293
4	11	10	5	-11.79	651.169
5	8	1	3	-12.68	431.627
6	9	10	3	-12.24	619.279
7	1	5.5	1	-12.45	317.215
8	3	5.5	5	-13.11	448.696
9	10	5.5	3	-13.45	594.632
10	2	5.5	3	-13.07	522.69
11	4	5.5	3	-13.73	**427.259**

Table S6. ANOVA table of the 2^3 full factorial design (DoE 1)

Factor		**F-value**	**p-Value**
ZP	Regression*	69.5167	0.000
	Lack of fit**	1.29146	0.464
Radius	Regression*	10.1686	0.022
	Lack of fit**	6.48271	0.279

*Significant at 5% probability ($p < 0.05$)

**Significant if $p > 0.05$

Table S7. ANOVA table of the central composite face-centered design (CCF; DoE 2)

Factor		F-value	p-Value
ZP	Regression*	8.51082	0.012
	Lack of fit**	0.78493	0.627
Radius	Regression*	22.5062	0.005
	Lack of fit**	0.37853	0.797

*Significant at 5% probability ($p < 0.05$)

**Significant if $p > 0.05$

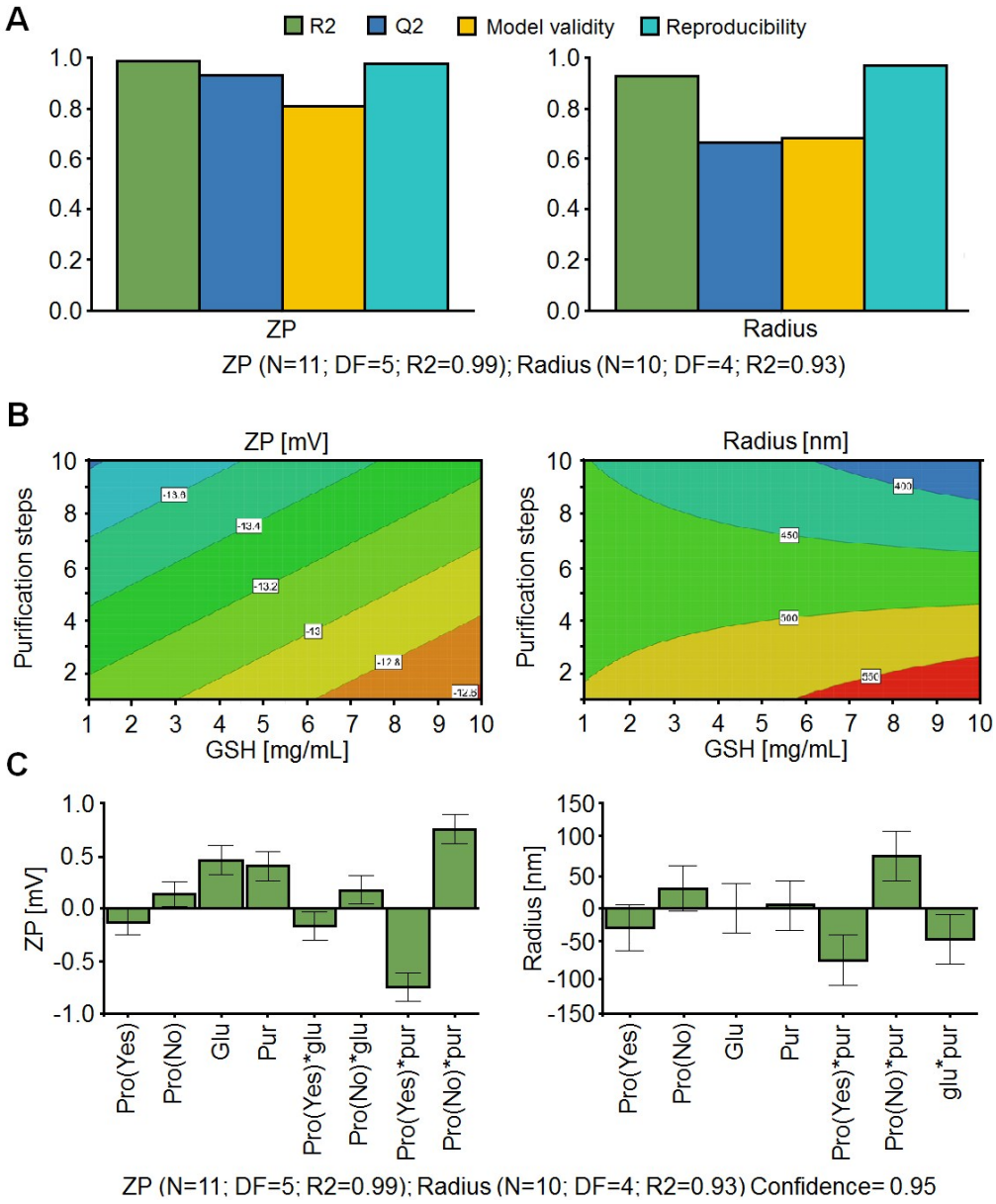

Figure S1. Optimization (Screening) of ultrasound assisted HSA/SF/GSH nanocapsules production via design of experiments (2^3 full factorial design). (A) Summary of fit plots for zeta potential (ZP, left) in mV and hydrodynamic particle radius (Radius, right) in nm including R^2 (goodness of fit), Q^2 (goodness of prediction), the model validity and the reproducibility based on three center points, whereby N indicates the number of experiments and DF refers to degrees of freedom. Model was fitted with MLR. (B) Response contour plots for zeta potential (ZP, left) in mV and hydrodynamic particle radius (Radius, right) in nm with constant protein addition (yes). (C) Extended coefficients plots of scaled and centered coefficients for zeta potential (ZP, left) in mV and hydrodynamic particle radius (Radius, right) in nm including significant 2 factor interactions, whereby R2 refers to goodness of fit, N indicates the number of experiments and DF refers to degrees of freedom. Coefficient plots were calculated using a confidence interval of 95%.

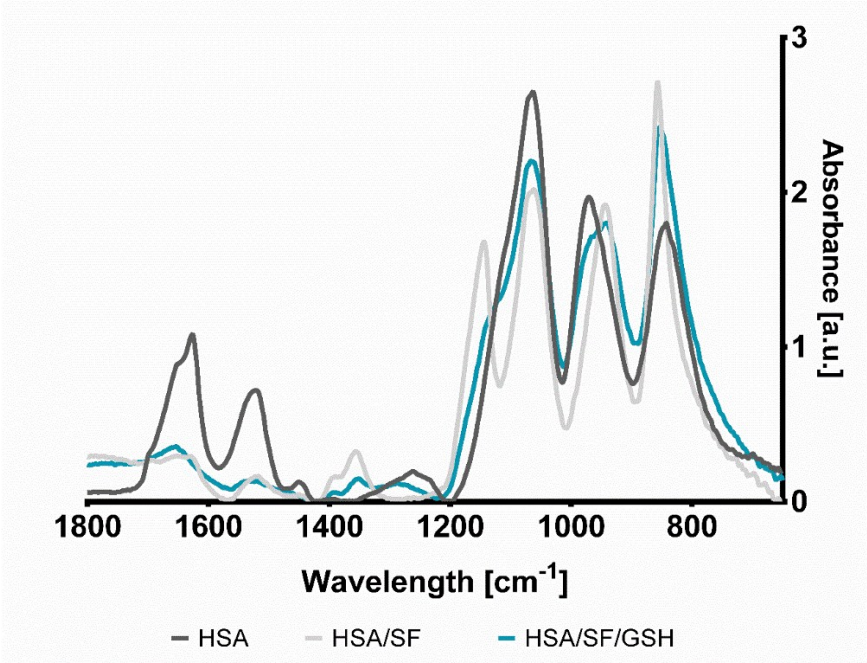

Figure S2: ATR-FTIR spectra of lyophilized HSA, HSA/SF and HSA/SF/GSH nanocapsules, normalized in the range of 650 to 1200 cm^{-1} and baseline corrected.

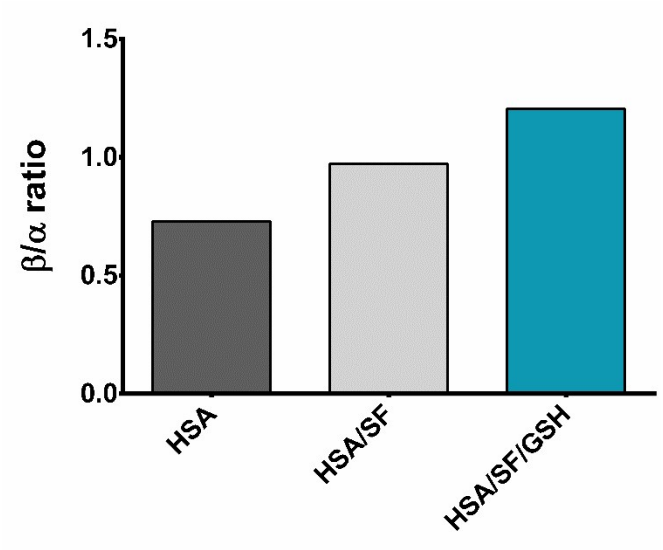

Figure S3: ATR-FTIR spectra based calculated β/α ratios of the Amid I bands (β:1627 cm^{-1}; α: 1648 cm^{-1}) of lyophilized HSA, HSA/SF and HSA/SF/GSH nanocapsules.

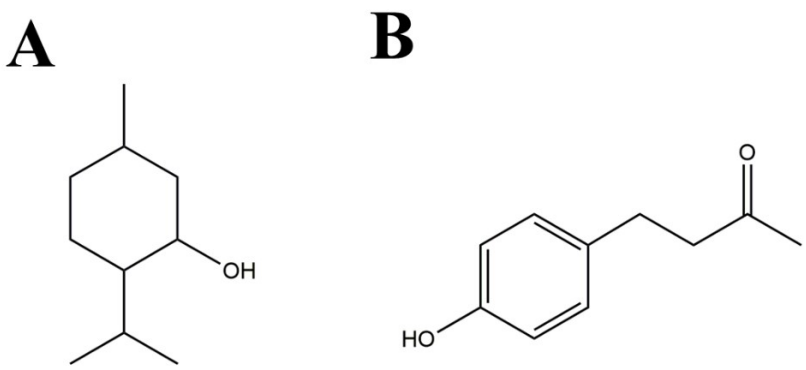

Figure S4. Chemical structures of (A) menthol (5-Methyl-2-(propan-2-yl)-cyclohexan-1-ol) and (B) raspberry ketone (4-(4-Hydroxyphenyl)butan-2-one)

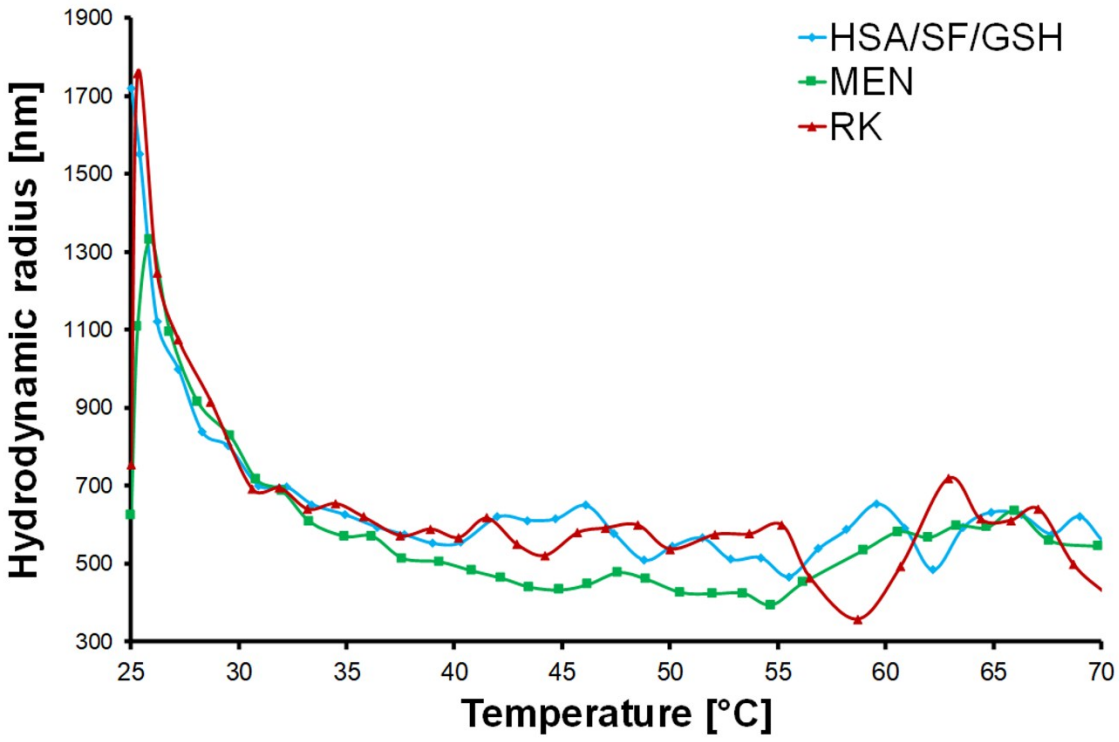

Figure S5. DLS based analysis of changes in hydrodynamic radius in nm over a temperature range of 25 to 70 °C of unloaded and MEN or RK loaded HSA/SF/GSH nanocapsules.

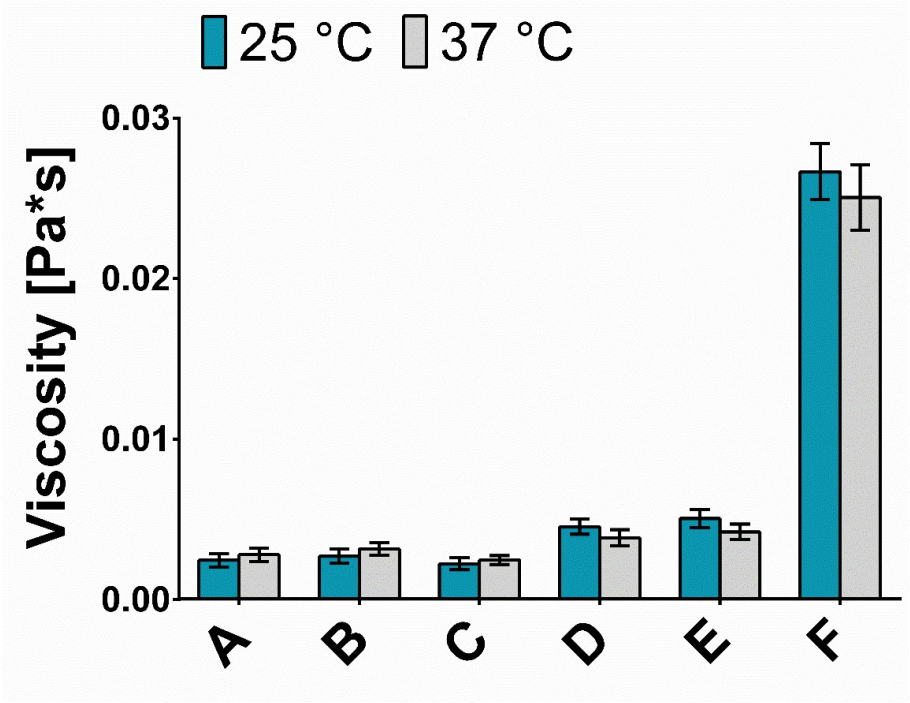

Figure S6. Viscosity values in Pa*s of different Artificial saliva (Tab. 1, A^{35}-B^{36} & D^{37}-E^{38}), including the commercial certified and normed artificial saliva by Pickering Laboratories (F) and the 100 mM sodium phosphate buffer pH 7.4 (C) at two different test temperatures (25 and 37 °C)